Geophys. J. Int. (2000) **143,** 319–327

Transient two-dimensional Kirchhoff diffraction of a plane elastic *SH* wave by a generalized linear-slip fracture*

Adrianus T. de Hoop

Laboratory of Electromagnetic Research, Delft University of Technology, Mekelweg 4, 2628 *CD Delft, the Netherlands. E-mail: a.t.dehoop@its.tudelft.nl*

Accepted 2000 June 11. Received 2000 June 9; in original form 2000 January 12

SUMMARY

Closed-form analytic time-domain expressions are obtained for the particle displacement of the total wave motion arising from the 2-D diffraction of a plane elastic *SH* wave by an imperfection of finite width in the interfacial bonding of two semi-infinite media. The properties of the imperfection are characterized by a matrix of 'spring coefficients' through which the traction on each of its two faces is linearly related to the particle displacement on either of the two faces. A boundary condition of this kind generalizes that of a linear-slip fracture. For this reason, the imperfection can be denoted as a 'generalized linear-slip fracture'. The Kirchhoff approximation is used to solve the diffraction problem. The time-domain expressions are obtained with the aid of the modified Cagniard method.

Key words: Kirchhoff diffraction, linear-slip fracture, *SH* wave, time domain.

1 INTRODUCTION

We investigate the 2-D transient plane elastic *SH*-wave scattering by an imperfection of finite width in the interfacial bonding of two semi-infinite media. The elastodynamic properties of the imperfection are described by a generalization of the linear-slip boundary condition that is used to describe the behaviour of an imperfect interface in the so-called displacement discontinuity model. For this reason the imperfection can be called a 'generalized linear-slip fracture'. The fracture is present in an unbounded, homogeneous, isotropic, perfectly elastic solid. The scattering problem is solved in the (modified) Kirchhoff approximation, which amounts to replacing the actual values of the dynamic traction and the particle displacement on both faces of the fracture by their values that would apply to the reflection and transmission of the incident plane wave by a fracture with the same elastodynamic properties, but of infinite width. The modified Cagniard method is used to obtain analytic closed-form expressions for the particle displacement of the different constituents from which the scattered wave motion is composed, that is, the geometrically reflected and transmitted plane waves and the cylindrical diffracted waves originating at the two edges of the fracture.

In a recent paper, Verweij & Chapman (1999) investigated the reflection and transmission of transient elastodynamic waves at a linear-slip interface. In their paper, reference to other literature on the use of linear-slip boundary conditions to describe the properties of fractures can be found.

The characterization of the elastodynamic properties of the fracture by the coefficients entering into the generalized linear-slip boundary condition opens the possibility of applying inverse-scattering optimization methods to reconstruct the properties of the fracture from observed scattered-wave data, expressed in terms of those coefficients. (For some general aspects of procedures of this kind, see De Hoop & De Hoop (2000).) This feature is of importance in the monitoring of the formation and identification of fractures in subsurface fossil energy reservoirs as well as in the quantitative non-destructive evaluation of mechanical structures.

2 DESCRIPTION OF THE CONFIGURATION

The scattering fracture is present in an unbounded, homogeneous, isotropic, perfectly elastic solid with volume density of mass ρ and Lamé stiffness coefficients λ and μ. The corresponding *SH*-wave speed is $c_S=(\mu/\rho)^{1/2}$. The position in the configuration is specified by the coordinates $\{x, y, z\}$ with respect to an orthogonal Cartesian reference frame with the origin $\mathcal{O}$ and the three mutually perpendicular base vectors $\{\mathbf{i}_x, \mathbf{i}_y, \mathbf{i}_z\}$, each of unit length. In the order indicated, the base vectors form a right-handed system. The time coordinate is t.

* Dedicated to Professor Leon Knopoff on the occasion of his 75th birthday.

Partial differentiation is denoted by ∂. The fracture is located at $\Sigma=\{a<x<b,\ -\infty<y<\infty,\ z=0\}$. The configuration is shown in Fig. 1. The particle displacement of the incident wave is parallel to the edges of the fracture. As a consequence, the scattering problem is 2-D, y-independent, in nature, and the scattered wave, too, is an *SH* wave with particle displacement parallel to the edges of the fracture.

The properties of the imperfection in interfacial bonding will be described by a generalized linear-slip boundary condition. A boundary condition of this type represents the imperfection ('generalized linear-slip fracture') locally as a linear, time-invariant, passive, lumped-element mechanical system where the traction at either of the two faces is homogeneously linearly related to the particle displacement at the two faces. The coefficients in this linear relation can be considered as types of *spring coefficients*. Physical constraints on these coefficients are that their values must satisfy the principle of reciprocity and that their matrix must be positive definite.

The scattering problem is solved in the (modified) Kirchhoff approximation. Furthermore, the modified Cagniard method (De Hoop 1958, 1960, 1988a,b; Achenbach 1973; Miklowitz 1978; Aki & Richards 1980) [actually an extension of it that has also been employed by Verweij & Chapman (1999)] is used to obtain closed-form analytic expressions for the different constituents from which the scattered wave is composed.

3 FORMULATION OF THE PROBLEM

The particle displacement $u_y=u_y(x, z, t)$ of the total elastic wave motion is written as the sum of the incident wave $u_y^{\mathrm{i}}=u_y^{\mathrm{i}}(x, z, t)$ and the scattered wave $u_y^{\mathrm{s}}=u_y^{\mathrm{s}}(x, z, t)$. The incident wave is the plane *SH* wave

$$u_y^{\mathrm{i}}=u_0(t-p_0x-\gamma_0z)\,, \tag{1}$$

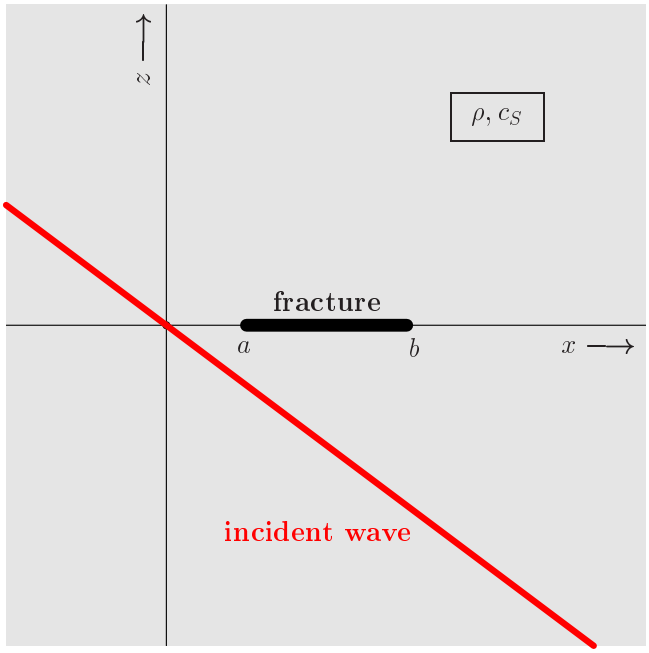

Figure 1. Diffracting generalized linear-slip fracture with incident plane *SH* wave.

in which p_0, with $-c_S^{-1}\le p_0\le c_S^{-1}$, is the incident-wave slowness along the x-direction,

$$\gamma_0=(c_S^{-2}-p_0^2)^{1/2}\ge 0 \tag{2}$$

is its slowness along the z-direction and $u_0=u_0(t)$ is the incident wave's time signature. The time coordinate is chosen such that $u_0(t)=0$ for $t<0$. The particle displacement of the scattered wave satisfies the 2-D scalar wave equation

$$(\partial_x^2+\partial_z^2-c_S^{-2}\partial_t^2)u_y^{\mathrm{s}}=0\quad\text{for }\{x, y, z\}\notin\Sigma\,. \tag{3}$$

The traction normal to planes parallel to the plane of the fracture is $\tau_{z,y}=\tau_{z,y}(x, z, t)$, with the incident-wave part $\tau_{z,y}^{\mathrm{i}}=\tau_{z,y}^{\mathrm{i}}(x, z, t)$ and the scattered-wave part $\tau_{z,y}^{\mathrm{s}}=\tau_{z,y}^{\mathrm{s}}(x, z, t)$. The stress/strain relation yields

$$\tau_{z,y}^{\mathrm{i,s}}=\mu\partial_z u_y^{\mathrm{i,s}}\quad\text{for }\{x, y, z\}\notin\Sigma\,. \tag{4}$$

The generalized linear-slip boundary condition used to characterize the elastodynamic properties of the fracture is taken as

$$\begin{bmatrix}-\tau_{z,y}(x, 0-, t)\\ \tau_{z,y}(x, 0+, t)\end{bmatrix}=\begin{bmatrix}C_{1,1} & C_{1,2}\\ C_{2,1} & C_{2,2}\end{bmatrix}\begin{bmatrix}u_y(x, 0-, t)\\ u_y(x, 0+, t)\end{bmatrix}, \tag{5}$$

where $0-$ is a shorthand notation for $\lim_{z\uparrow 0}$ and $0+$ is a shorthand notation for $\lim_{z\downarrow 0}$. The coefficients in this relation can be considered as types of *spring coefficients*, which are quantitative representation of the properties of the fracture considered as a linear elastostatic system. In view of the principle of reciprocity, we have

$$C_{1,2}=C_{2,1}\,, \tag{6}$$

while the property of passivity leads to the conditions

$$C_{1,1}>0\,,\quad C_{2,2}>0\,,\quad \begin{vmatrix}C_{1,1} & C_{1,2}\\ C_{2,1} & C_{2,2}\end{vmatrix}>0\,. \tag{7}$$

The values $C_{1,1}=C_{1,2}=C_{2,1}=C_{2,2}=0$ yield the case where, on both faces of the crack, the traction vanishes, while the values $C_{1,1}=-C_{1,2}=-C_{2,1}=C_{2,2}$ yield the case considered by Verweij & Chapman (1999) of an interface characterized by a linear-slip boundary condition.

The scattered wave is, via the scattering by the fracture, causally related to the incident wave. This implies that the scattered wave vanishes prior to the instant at which the incident wave hits the fracture (which is the instant $\min(p_0a, p_0b)$).

4 DETERMINATION OF THE COMPLEX SLOWNESS PLANE SCATTERED-WAVE AMPLITUDES

The problem will be solved with the aid of (an extension of) the modified Cagniard method. In this method, first the Laplace transformation with respect to time is carried out. To show the notation, we give the expression for the transform of the incident wave's signature,

$$\hat{u}_0(s)=\int_{t=0}^{\infty}\exp(-st)u_0(t)\,dt\,. \tag{8}$$

For the physically interesting case of bounded incident-wave signatures, the right-hand side of eq. (8) exists in the right half $\{s\in\mathbb{C};\ \Re e(s)>0\}$ of the complex s-plane, where it is a regular analytic function of the *complex frequency* s. Lerch's theorem

of the one-sided Laplace transformation (Widder 1946) states that a causal time function belonging to a class of functions that encompasses the one we have specified is related one-to-one to its Laplace transform at the equidistant set of points $\{s \in \mathscr{R};\ s=s_0+nh,\ s_0>0,\ h>0,\ n=0,\ 1,\ 2,\ \ldots\}$ on the positive real s-axis. With this property in mind, the Laplace transform parameter s will, throughout our analysis, be restricted to real, positive values.

The Laplace-transformed incident-wave particle displacement is then given by

$$\hat{u}_y^{\mathrm{i}}(x,z,s)=\hat{u}_0(s)\exp[-s(p_0x+\gamma_0 z)]\,. \tag{9}$$

The Laplace-transformed scattered-wave particle displacement is represented as the system of complex slowness integrals

$$\hat{u}_y^{\mathrm{s}}(x,\,z,\,s)=\frac{\hat{u}_0(s)}{2\pi\mathrm{i}}\int_{p=-\mathrm{i}\infty}^{\mathrm{i}\infty}A^-(p,\,s)\exp\{-s[px-\gamma_S(p)z]\}\,dp \quad \text{for } z<0\,, \tag{10}$$

$$\hat{u}_y^{\mathrm{s}}(x,\,z,\,s)=\frac{\hat{u}_0(s)}{2\pi\mathrm{i}}\int_{p=-\mathrm{i}\infty}^{\mathrm{i}\infty}A^+(p,\,s)\exp\{-s[px+\gamma_S(p)z]\}\,dp \quad \text{for } z>0\,. \tag{11}$$

Here, i is the imaginary unit and

$$\gamma_S=(c_S^{-2}-p^2)^{1/2} \quad \text{with} \quad \mathscr{R}e(\gamma_S)\geq 0 \text{ for all } p\in\mathscr{C}\,. \tag{12}$$

[Note that, in view of eq. (2), $\gamma_S(p_0)=\gamma_0$.] The corresponding representation for the traction normal to the planes parallel to the plane of the fracture follows from eqs (4) and (9)–(11) as

$$\hat{\tau}_{z,y}^{\mathrm{i}}(x,\,z,\,s)=-\mu s\gamma_0\hat{u}_0(s)\exp[-s(p_0x+\gamma_0 z)]\,, \tag{13}$$

while

$$\hat{\tau}_{z,y}^{\mathrm{s}}(x,\,z,\,s)=\frac{\mu s\hat{u}_0(s)}{2\pi\mathrm{i}}\int_{p=-\mathrm{i}\infty}^{\mathrm{i}\infty}\gamma_S(p)A^-(p,\,s)\times\exp\{-s[px-\gamma_S(p)z]\}\,dp \quad \text{for } z<0\,, \tag{14}$$

$$\hat{\tau}_{z,y}^{\mathrm{s}}(x,\,z,\,s)=-\frac{\mu s\hat{u}_0(s)}{2\pi\mathrm{i}}\int_{p=-\mathrm{i}\infty}^{\mathrm{i}\infty}\gamma_S(p)A^+(p,\,s)\times\exp\{-s[px+\gamma_S(p)z]\}\,dp \quad \text{for } z>0\,. \tag{15}$$

The complex slowness plane amplitude coefficients $A^-(p,\,s)$ and $A^+(p,\,s)$ remain to be determined from the boundary conditions in the plane $\{z=0\}$ of the fracture. Across the perfectly bonded part of this plane, both the particle displacement and the traction are continuous. Across the fracture these quantities jump by finite amounts. For the latter, we substitute the values that follow from the plane wave reflection and transmission at a planar interface to which the boundary conditions of eq. (5) apply (*Kirchhoff approximation*). Accordingly, we write

$$\hat{u}_y(x,\,0-,\,s)=[1+\hat{R}(p_0,\,s)]\hat{u}_0(s)\exp(-sp_0x) \quad \text{for } a<x<b\,, \tag{16}$$

$$\hat{u}_y(x,\,0+,\,s)=\hat{T}(p_0,\,s)\hat{u}_0(s)\exp(-sp_0x) \quad \text{for } a<x<b\,, \tag{17}$$

and

$$\hat{\tau}_{z,y}(x,\,0-,\,s)=-s\mu\gamma_0[1-\hat{R}(p_0,\,s)]\hat{u}_0(s)\exp(-sp_0x) \quad \text{for } a<x<b\,, \tag{18}$$

$$\hat{\tau}_{z,y}(x,\,0+,\,s)=-s\mu\gamma_0\hat{T}(p_0,\,s)\hat{u}_0(s)\exp(-sp_0x) \quad \text{for } a<x<b\,, \tag{19}$$

in which $\hat{R}(p_0,\,s)$ is the plane wave particle-displacement reflection coefficient and $\hat{T}(p_0,\,s)$ is the plane wave particle-displacement transmission coefficient, both for a fracture of the type under consideration, but of infinite extent. The complex slowness representations for the jumps

$$\hat{u}_y(x,\,0+,\,s)-\hat{u}_y(x,\,0-,\,s)=[\hat{T}(p_0,\,s)-1-\hat{R}(p_0,\,s)]\frac{\hat{u}_0(s)}{2\pi\mathrm{i}}\times\int_{p=-\mathrm{i}\infty}^{\mathrm{i}\infty}\exp(-spx)\frac{\exp[s(p-p_0)b]-\exp[s(p-p_0)a]}{p-p_0}\,dp \tag{20}$$

and

$$\hat{\tau}_{z,y}(x,\,0+,\,s)-\hat{\tau}_{z,y}(x,\,0-,\,s)=-s\mu\gamma_0[\hat{T}(p_0,\,s)-1+\hat{R}(p_0,\,s)]\,\frac{\hat{u}_0(s)}{2\pi\mathrm{i}}\times\int_{p=-\mathrm{i}\infty}^{\mathrm{i}\infty}\exp(-spx)\,\frac{\exp[s(p-p_0)b]-\exp[s(p-p_0)a]}{p-p_0}\,dp \tag{21}$$

do reproduce the jump conditions following from eqs (16)–(19), as can be verified by supplementing the path of integration in the complex p-plane with semi-circular arcs at infinity in accordance with Jordan's lemma, and applying the theorem of residues.

Combining eqs (9)–(11) with eq. (20) and eqs (13)–(15) with eq. (21), and observing that the resulting identities hold on the entire interval $-\infty<x<\infty$, we arrive at the relations

$$A^+(p,\,s)-A^-(p.s)=[\hat{T}(p_0,\,s)-1-\hat{R}(p_0,\,s)]\,\frac{\exp[s(p-p_0)b]-\exp[s(p-p_0)a]}{p-p_0} \tag{22}$$

and

$$-\gamma_S(p)[A^+(p,\,s)+A^-(p,\,s)]=-\gamma_0[\hat{T}(p_0,\,s)-1+\hat{R}(p_0,\,s)]\times\frac{\exp[s(p-p_0)b]-\exp[s(p-p_0)a]}{p-p_0}\,. \tag{23}$$

From this we obtain

$$A^-(p,s)=\frac{1}{2}\Big\{-\hat{T}(p_0,s)+1+\hat{R}(p_0,s)+\frac{\gamma_0}{\gamma_S(p)}\,[\hat{T}(p_0,s)-1+\hat{R}(p_0,s)]\Big\}\times\frac{\exp[s(p-p_0)b]-\exp[s(p-p_0)a]}{p-p_0} \tag{24}$$

and

$$A^+(p,s)=\frac{1}{2}\Big\{\hat{T}(p_0,s)-1-\hat{R}(p_0,s)+\frac{\gamma_0}{\gamma_S(p)}\,[\hat{T}(p_0,s)-1+\hat{R}(p_0,s)]\Big\}\times\frac{\exp[s(p-p_0)b]-\exp[s(p-p_0)a]}{p-p_0}\,. \tag{25}$$

In Section 5, the plane wave, planar-interface reflection coefficient $\hat{R}(p_0, s)$ and the plane wave, planar-interface transmission coefficient $\hat{T}(p_0, s)$ will be determined. In Section 6, the transformation back to the time domain will be carried out.

5 ANALYSIS OF THE PLANE *SH*-WAVE REFLECTION AND TRANSMISSION BY A GENERALIZED LINEAR-SLIP FRACTURE OF INFINITE EXTENT

To analyse the plane *SH*-wave reflection and transmission by a generalized linear-slip interface of infinite extent, we use for the Laplace transform of the particle displacement the representation

$$\hat{u}_y=\hat{u}_y^{\mathrm{i}}+\hat{u}_y^{\mathrm{r}}\quad\text{for } z<0\,, \tag{26}$$

$$\hat{u}_y=\hat{u}_y^{\mathrm{t}}\quad\text{for } z>0\,, \tag{27}$$

in which the incident wave $\hat{u}^{\mathrm{i}}$ is again given by eq. (9). For the reflected wave $\hat{u}^{\mathrm{r}}$ we have, in accordance with eq. (16),

$$\hat{u}_y^{\mathrm{r}}=\hat{R}(p_0,s)\hat{u}_0(s)\exp[-s(p_0x-\gamma_0z)]\,, \tag{28}$$

and for the transmitted wave, in accordance with eq. (17),

$$\hat{u}_y^{\mathrm{t}}=\hat{T}(p_0,s)\hat{u}_0(s)\exp[-s(p_0x+\gamma_0z)]\,. \tag{29}$$

The corresponding representation for the Laplace transform of the traction normal to the planes parallel to the plane of the fracture is

$$\hat{\tau}_{z,y}=\hat{\tau}_{z,y}^{\mathrm{i}}+\hat{\tau}_{z,y}^{\mathrm{r}}\quad\text{for } z<0\,, \tag{30}$$

$$\hat{\tau}_{z,y}=\hat{\tau}_{z,y}^{\mathrm{t}}\quad\text{for } z>0\,, \tag{31}$$

in which

$$\hat{\tau}_{z,y}^{\mathrm{i}}=-\mu s\gamma_0\hat{u}_0(s)\exp[-s(p_0x+\gamma_0z)] \tag{32}$$

and

$$\hat{\tau}_{z,y}^{\mathrm{r}}=\mu s\gamma_0\hat{R}(p_0,s)\hat{u}_0(s)\exp[-s(p_0x-\gamma_0z)]\,, \tag{33}$$

$$\hat{\tau}_{z,y}^{\mathrm{t}}=-\mu s\gamma_0\hat{T}(p_0,s)\hat{u}_0(s)\exp[-s(p_0x+\gamma_0z)]\,. \tag{34}$$

Substitution of these representations in the boundary conditions (5) yields

$$\mu s\gamma_0[1-\hat{R}(p_0,s)]=C_{1,1}[1+\hat{R}(p_0,s)]+C_{1,2}\hat{T}(p_0,s)\,, \tag{35}$$

$$-\mu s\gamma_0\hat{T}(p_0,s)]=C_{2,1}[1+\hat{R}(p_0,s)]+C_{2,2}\hat{T}(p_0,s)\,. \tag{36}$$

From these equations we obtain

$$\hat{R}(p_0,s)=1-\frac{2(\mu s\gamma_0C_{1,1}+C_{1,1}C_{2,2}-C_{1,2}C_{2,1})}{\Delta_C(s)}\,, \tag{37}$$

$$\hat{T}(p_0,s)=-\frac{2\mu s\gamma_0C_{2,1}}{\Delta_C(s)}\,, \tag{38}$$

in which

$$\Delta_C(s)=(\mu s\gamma_0+C_{1,1})(\mu s\gamma_0+C_{2,2})-C_{1,2}C_{2,1}\,. \tag{39}$$

For $\gamma_0=0$ (grazing incidence), i.e. for $p_0=\pm c_S^{-1}$, we obtain $\hat{R}(p_0, s)=-1$ and $\hat{T}(p_0, s)=0$, which yields $\hat{u}_y^{\mathrm{r}}=-\hat{u}_y^{\mathrm{i}}$ and $\hat{u}_y^{\mathrm{t}}=0$, hence $u_y^{\mathrm{r}}=-u_y^{\mathrm{i}}$ and $u_y^{\mathrm{t}}=0$. For $\gamma_0\neq0$, i.e. for $p_0\neq\pm c_S^{-1}$, we rewrite the right-hand sides of eqs (37) and (38) as their partial-fraction decompositions. To this end, eq. (39) is rewritten as

$$\Delta_C(s)=(\mu\gamma_0)^2(s+\alpha)(s+\beta)\,, \tag{40}$$

with

$$\alpha=\frac{1}{\mu\gamma_0}\left\{\frac{C_{1,1}+C_{2,2}}{2}-\left[\left(\frac{C_{1,1}+C_{2,2}}{2}\right)^2-\Big(C_{1,1}C_{2,2}-C_{1,2}C_{2,1}\Big)\right]^{1/2}\right\}, \tag{41}$$

$$\beta=\frac{1}{\mu\gamma_0}\left\{\frac{C_{1,1}+C_{2,2}}{2}+\left[\left(\frac{C_{1,1}+C_{2,2}}{2}\right)^2-(C_{1,1}C_{2,2}-C_{1,2}C_{2,1})\right]^{1/2}\right\}. \tag{42}$$

It is easily verified that, in view of the conditions laid upon the fracture's spring coefficients, both α and β are real valued. For the reflection coefficient the partial-fraction decomposition leads to

$$\hat{R}(p_0,s)=1-\frac{R_\alpha}{s+\alpha}+\frac{R_\beta}{s+\beta}\,, \tag{43}$$

with

$$R_\alpha=\frac{2(-\mu\gamma_0\alpha C_{1,1}+C_{1,1}C_{2,2}-C_{1,2}C_{2,1})}{(\mu\gamma_0)^2(\beta-\alpha)} \tag{44}$$

and

$$R_\beta=\frac{2(-\mu\gamma_0\beta C_{1,1}+C_{1,1}C_{2,2}-C_{1,2}C_{2,1})}{(\mu\gamma_0)^2(\beta-\alpha)}\,, \tag{45}$$

and for the transmission coefficient to

$$\hat{T}(p_0,s)=\frac{T_\alpha}{s+\alpha}-\frac{T_\beta}{s+\beta}\,, \tag{46}$$

with

$$T_\alpha=\frac{2\alpha C_{2,1}}{\mu\gamma_0(\beta-\alpha)} \tag{47}$$

and

$$T_\beta = \frac{2\beta C_{2,1}}{\mu\gamma_0(\beta-\alpha)}\,. \tag{48}$$

Inverse Laplace transformation of eq. (43) leads to the *time-domain reflection function*,

$$R(p_0, t) = \delta(t) - R_\alpha \exp(-\alpha t)H(t) + R_\beta \exp(-\beta t)H(t)\,, \tag{49}$$

where $\delta(t)$ is the Dirac distribution and $H(t)$ is the Heaviside unit step function. Inverse Laplace transformation of eq. (46) leads to the *time-domain transmission function*,

$$T(p_0, t) = T_\alpha \exp(-\alpha t)H(t) - T_\beta \exp(-\beta t)H(t)\,. \tag{50}$$

The time-domain expressions corresponding to eqs (28) and (29) are finally obtained as

$$u_y^{\rm r}(x, z, t) = u_0(t) \overset{(t-p_0x+\gamma_0z)}{*} R(p_0, t) \tag{51}$$

and

$$u_y^{\rm t}(x, z, t) = u_0(t) \overset{(t-p_0x-\gamma_0z)}{*} T(p_0, t)\,, \tag{52}$$

where $\overset{(t)}{*}$ denotes convolution with respect to time.

6 TRANSFORMATION BACK TO THE TIME DOMAIN

In this section, the Laplace-transformed scattered-wave particle displacement will be transformed back to the time domain through the application of (an extension of) the modified Cagniard method. The starting point is the representations (9)–(11), in which for the complex slowness domain scattered-wave amplitudes $A^-(p_0, s)$ and $A^+(p_0, s)$ the expressions (24) and (25) are substituted, while for the plane wave reflection coefficient $\hat{R}(p_0, s)$ the expression (43) and for the plane wave transmission coefficient $\hat{T}(p_0, s)$ the expression (46) are used.

The principal step consists of replacing the original path of integration in the complex p-plane (the imaginary axis) by a path along which the exponential functions in the integrands take the form $\exp(-s\tau)$, where τ is a real variable of integration. Once this has been accomplished, the application of Lerch's theorem in conjunction with some elementary rules of the one-sided Laplace transformation suffice to construct the final time-domain expressions for the particle displacement. As far as the edge diffraction effects are concerned, the building blocks in these expressions are the half-plane Kirchhoff diffraction function $D_{\rm K}^{\rm I} = D_{\rm K}^{\rm I}(x, z, t)$ associated with the causal 2-D scattering of an incident plane scalar wave with a Dirac delta pulse signature by a semi-infinite screen on which the Dirichlet boundary condition (vanishing wave function) holds (first boundary value problem) and the half-plane Kirchhoff diffraction function $D_{\rm K}^{\rm II} = D_{\rm K}^{\rm II}(x, x, t)$ associated with the causal 2-D scattering of an incident plane scalar wave with a Dirac delta pulse signature by a semi-infinite screen on which the Neumann boundary condition (vanishing normal derivative of the wave function) holds (second boundary value problem).

The complex slowness domain representation of $\hat{D}_{\rm K}^{\rm I}$ is given by (De Hoop 1958, p. 42)

$$\hat{D}_{\rm K}^{\rm I}(x, z, s) = \frac{1}{2\pi{\rm i}} \int_{p=-{\rm i}\infty}^{{\rm i}\infty} \frac{\gamma_0}{\gamma_S(p)} \frac{1}{p-p_0} \exp\{-s[px+\gamma_S(p)|z|]\}\, dp$$
$$\text{for } \mathscr{R}e(p_0) > 0. \tag{53}$$

This expression also follows from eqs (24) and (25) through the values of $A^-(p, s) = A^+(p, s)$ corresponding to $\hat{R}(p_0, s) = -1$, $\hat{T}(p_0, s) = 0$, $a = 0$, $b \to \infty$ and $p_0 > 0$.

The complex slowness domain representation of $\hat{D}_{\rm K}^{\rm II}$ is given by (De Hoop 1958, p. 43)

$$\hat{D}_{\rm K}^{\rm II}(x, z, s) = {\rm sign}(z) \frac{1}{2\pi{\rm i}} \int_{p=-{\rm i}\infty}^{{\rm i}\infty} \frac{1}{p-p_0} \exp\{-s[px+\gamma_S(p)|z|]\}\, dp$$
$$\text{for } \mathscr{R}e(p_0) > 0\,. \tag{54}$$

This expression also follows from eqs (24) and (25) through the values of $A^-(p, s) = -A^+(p, s)$ corresponding to $\hat{R}(p_0, s) = 1$, $\hat{T}(p_0, s) = 0$, $a = 0$, $b \to \infty$ and $p_0 > 0$.

With these provisions, the expressions (9)–(11) for $\hat{u}_y^{\rm s}$ can be combined as follows:

$$\begin{aligned}\hat{u}_y^{\rm s}(x, z, s) = {} & \frac{1}{2}\,\hat{u}_0(s)\exp(-sp_0a) \\ & \times\{[-\hat{T}(p_0, s)+1-\hat{R}(p_0, s)]\hat{D}_{\rm K}^{\rm I}(x-a, z, s) \\ & +[-\hat{T}(p_0, s)+1+\hat{R}(p_0, s)]\hat{D}_{\rm K}^{\rm II}(x-a, z, s)\} \\ & -\frac{1}{2}\,\hat{u}_0(s)\exp(-sp_0b) \\ & \times\{[-\hat{T}(p_0, s)+1-\hat{R}(p_0, s)]\hat{D}_{\rm K}^{\rm I}(x-b, z, s) \\ & +[-\hat{T}(p_0, s)+1+\hat{R}(p_0, s)]\hat{D}_{\rm K}^{\rm II}(x-b, z, s)\}\,.\end{aligned} \tag{55}$$

The first term in braces on the right-hand side is representative of the scattering effects of the left edge of the fracture, and the second term in braces is representative of the scattering effects of the right edge of the fracture. Transformation back to the time domain leads to

$$\begin{aligned}u_y^{\rm s}(x, z, t) = {} & \frac{1}{2}\,u_0(t-p_0a) \overset{(t)}{*} \{[-T(p_0, t)+\delta(t) \\ & -R(p_0, t)] \overset{(t)}{*} D_{\rm K}^{\rm I}(x-a, z, t) \\ & +[-T(p_0, t)+\delta(t)+R(p_0, t)] \overset{(t)}{*} D_{\rm K}^{\rm II}(x-a, z, t)\} \\ & -\frac{1}{2}\,u_0(t-p_0b) \overset{(t)}{*} \{[-T(p_0, t)+\delta(t) \\ & -R(p_0, t)] \overset{(t)}{*} D_{\rm K}^{\rm I}(x-b, z, t) \\ & +[-T(p_0, t)+\delta(t)+R(p_0, t)] \overset{(t)}{*} D_{\rm K}^{\rm II}(x-b, z, t)\}\,,\end{aligned} \tag{56}$$

in which (see Appendix A)

$$D_{\rm K}^{\rm I}(x, z, t) = D_{\rm K}^{\rm I;ray}(x, z, t) + D_{\rm K}^{\rm I;d}(x, z, t)\,, \tag{57}$$

with the ray-geometrical contribution

$$D_{\rm K}^{\rm I;ray}(x, z, t) = -\left\{0, \frac{1}{2}, 1\right\}\delta(t-p_0x-\gamma_0|z|)$$
$$\text{for } \{x/R < p_0c_S,\ x/R = p_0c_S,\ x/R > p_0c_S\} \tag{58}$$

and the diffraction contribution

$$D_{\rm K}^{\rm I;d}(x, z, t) = \frac{1}{\pi}\,\mathscr{R}e\left[\frac{\gamma_S(p_S)}{p_S-p_0}\right]\frac{1}{(t^2-T_S^2)^{1/2}}\,H(t-T_S)\,, \tag{59}$$

while

$$D_{\mathrm{K}}^{\mathrm{II}}(x,z,t)=D_{\mathrm{K}}^{\mathrm{II;ray}}(x,z,t)+D_{\mathrm{K}}^{\mathrm{II;d}}(x,z,t)\,, \tag{60}$$

with the ray-geometrical contribution

$$D_{\mathrm{K}}^{\mathrm{II;ray}}(x,z,t)=-\mathrm{sign}(z)\left\{0,\frac{1}{2},1\right\}\delta(t-p_0x-\gamma_0|z|)$$
$$\text{for } \{x/R<p_0c_S,\ x/R=p_0c_S,\ x/R>p_0c_S\} \tag{61}$$

and the diffraction contribution

$$D_{\mathrm{K}}^{\mathrm{II;d}}(x,z,t)=\mathrm{sign}(z)\,\frac{1}{\pi}\,\mathscr{R}e\left[\frac{\gamma_0}{p_S-p_0}\right]\frac{1}{(t^2-T_S^2)^{1/2}}\,H(t-T_S)\,. \tag{62}$$

In these expressions

$$R=(x^2+z^2)^{1/2}\,;\quad T_S=T_S(x,z)=R/c_S\,, \tag{63}$$

with R the distance from the diffracting edge to the point of observation and T_S the S-wave traveltime from the diffracting edge to the point of observation.

To express in a concise manner the structure of the different wavefield constituents in the different regions of space where they manifest themselves, we introduce the notation

$$R^a=[(x-a)^2+z^2]^{1/2} \tag{64}$$

and

$$T_S^a=R^a/c_S \tag{65}$$

for the distance and the S-wave traveltime, respectively, from the left edge of the fracture to the point of observation, together with

$$R^b=[(x-b)^2+z^2]^{1/2} \tag{66}$$

and

$$T_S^b=R^b/c_S \tag{67}$$

for the distance and the S-wave traveltime, respectively, from the right edge of the fracture to the point of observation. In relation to the spatial support of the ray-geometrically reflected part of the scattered wavefield we introduce the domain

$$\mathscr{D}^{\mathrm{r}}=\{a+(p_0/\gamma_0)|z|<x<b+(p_0/\gamma_0)|z|,\ -\infty<y<\infty,\ z<0\}\,, \tag{68}$$

its boundary,

$$\partial\mathscr{D}^{\mathrm{r}}=\{x=a+(p_0/\gamma_0)|z|,\ -\infty<y<\infty,\ z<0\}$$
$$\cup\{x=b+(p_0/\gamma_0)|z|,\ -\infty<y<\infty,\ z<0\}\,, \tag{69}$$

and the complement of the closure of $\mathscr{D}^{\mathrm{r}}\cup\partial\mathscr{D}^{\mathrm{r}}$ in $\mathscr{R}^3$,

$$\mathscr{D}^{r'}=\{-\infty<x<a+(p_0/\gamma_0)|z|,\ -\infty<y<\infty,\ z<0\}$$
$$\cup\{b+(p_0/\gamma_0)|z|<x<\infty,\ -\infty<y<\infty,\ z<0\}\,. \tag{70}$$

Similarly, in relation to the spatial support of the ray-geometrically transmitted part of the scattered wavefield we introduce the domain

$$\mathscr{D}^{\mathrm{t}}=\{a+(p_0/\gamma_0)|z|<x<b+(p_0/\gamma_0)|z|,\ -\infty<y<\infty,\ z>0\}\,, \tag{71}$$

its boundary,

$$\partial\mathscr{D}^{\mathrm{t}}=\{x=a+(p_0/\gamma_0)|z|,\ -\infty<y<\infty,\ z>0\}$$
$$\cup\{x=b+(p_0/\gamma_0)|z|,\ -\infty<y<\infty,\ z>0\}\,, \tag{72}$$

and the complement of the closure of $\mathscr{D}^{\mathrm{t}}\cup\partial\mathscr{D}^{\mathrm{t}}$ in $\mathscr{R}^3$,

$$\mathscr{D}^{t'}=\{-\infty<x<a+(p_0/\gamma_0)|z|,\ -\infty<y<\infty,\ z>0\}$$
$$\cup\{b+(p_0/\gamma_0)|z|<x<\infty,\ -\infty<y<\infty,\ z>0\}\,. \tag{73}$$

With these preliminaries, the particle displacement of the total wave motion as obtained from eq. (56) takes the form (Fig. 2)

$$u_y=u_y^{\mathrm{i}}+u_y^{\mathrm{ray;r}}+u_y^{\mathrm{ray;t}}+u_y^{\mathrm{d;a}}+u_y^{\mathrm{d;b}}, \tag{74}$$

in which the *ray-geometrical reflected part* of the scattered wave is obtained as

$$u_y^{\mathrm{ray;r}}(x,z,t)=\left\{1,\frac{1}{2},0\right\}u_0(t)\ \overset{(t-p_0x+\gamma_0z)}{*}\ R(p_0,t)$$
$$\text{for } \{x,y,z\}\in\{\mathscr{D}^{\mathrm{r}},\partial\mathscr{D}^{\mathrm{r}},\mathscr{D}^{r'}\}\,, \tag{75}$$

the *ray-geometrical transmitted part* of the scattered wave as

$$u_y^{\mathrm{ray;t}}(x,z,t)=-u_y^{\mathrm{i}}(x,z,t)+\left\{1,\frac{1}{2},0\right\}u_0(t)\ \overset{(t-p_0x-\gamma_0z)}{*}\ T(p_0,t)$$
$$\text{for } \{x,y,z\}\in\{\mathscr{D}^{\mathrm{t}},\partial\mathscr{D}^{\mathrm{t}},\mathscr{D}^{t'}\}\,, \tag{76}$$

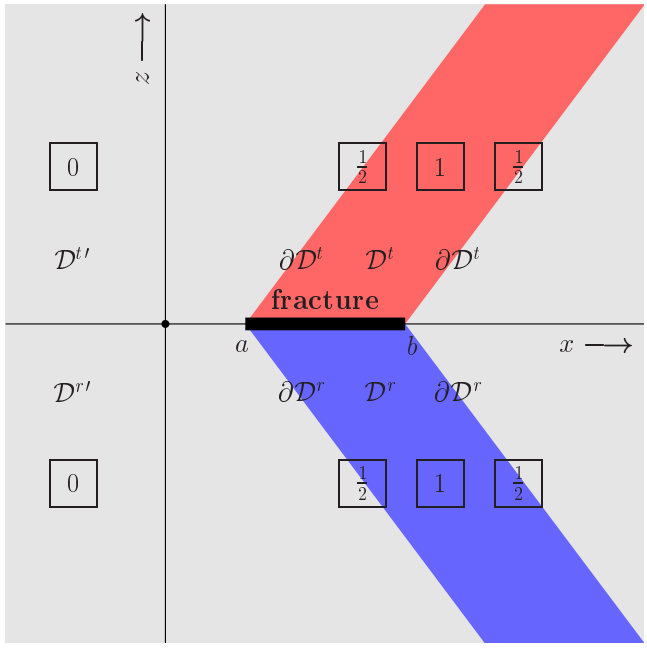

Figure 2. The ray-geometrically reflected and transmitted wave contributions.

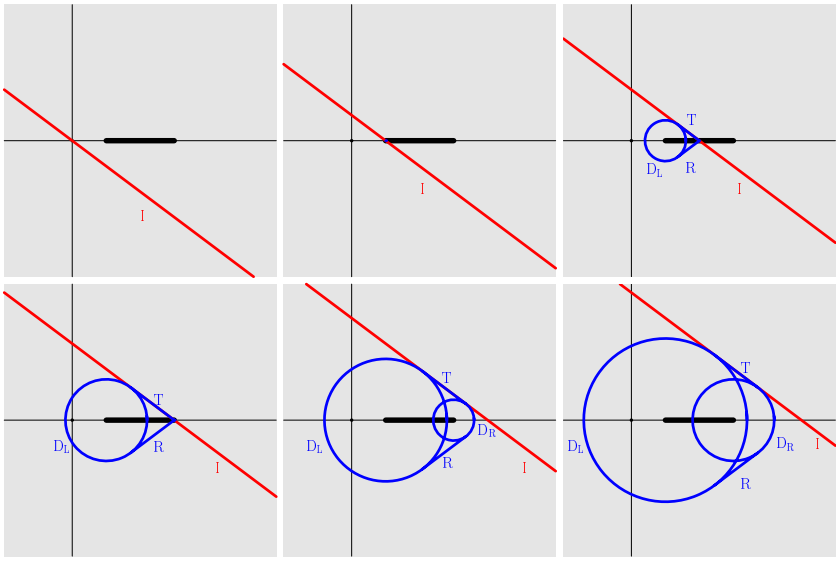

Figure 3. Wavefront snapshots showing the incident wave (I), the reflected wave (R), the transmitted wave (T), the diffracted wave left edge (D_L) and the diffracted wave right edge (D_R).

the *left-edge diffracted part* of the scattered wave as

$$u_y^{\mathrm{d;a}}(x,z,t)=\frac{1}{2}\,u_0(t-p_0a)\overset{(t)}{*}\{[-T(p_0,t)+\delta(t)-R(p_0,t)]\overset{(t)}{*}D_{\mathrm{K}}^{\mathrm{I;d}}(x-a,z,t)+[-T(p_0,t)+\delta(t)+R(p_0,t)]\overset{(t)}{*}D_{\mathrm{K}}^{\mathrm{II;a}}(x-a,z,t)\} \tag{77}$$

and the *right-edge diffracted part* of the scattered wavefield as

$$u_y^{\mathrm{d;b}}(x,z,t)=\frac{1}{2}\,u_0(t-p_0b)\overset{(t)}{*}\{[-T(p_0,t)+\delta(t)-R(p_0,t)]\overset{(t)}{*}D_{\mathrm{K}}^{\mathrm{I;d}}(x-b,z,t)+[-T(p_0,t)+\delta(t)+R(p_0,t)]\overset{(t)}{*}D_{\mathrm{K}}^{\mathrm{II;b}}(x-b,z,t)\}\,. \tag{78}$$

For points of observation on ∂D^{r} and ∂D^{t}, the expressions for the left- and right-edge diffracted parts of the scattered wavefield have, as the derivation in Appendix A shows, near their arrival times to be interpreted as their limiting values approached from behind their wave fronts.

With this, the derivation of closed-form expressions for the scattered wavefield has been completed. Fig. 3 shows some time snaps of the total wave fronts at equidistant successive snap times.

7 CONCLUSIONS

A closed-form analytic expression has been derived for the 2-D time-domain scattering of a plane elastic *SH* wave by a generalized linear-slip fracture of finite width in the Kirchhoff approximation. The properties of the fracture (an imperfection in the interfacial bonding of two semi-infinite media) are described in terms of a matrix of 'spring coefficients'. The relevant condition expresses the traction on either face of the fracture in terms of the particle displacement on its two faces. The *spring coefficients* are representative of the 'stiffness' of the imperfection. The solution of the scattering problem could provide a first step towards the creation of a parameter inversion analysis that aims at characterizing the properties of an imperfection in the realm of fracture detection and monitoring in subsurface fossil energy reservoirs as well as in the quantitative non-destructive evaluation of mechanical structures.

ACKNOWLEDGMENTS

Prof. Michael A. Slawinsky of the University of Calgary, Department of Geology & Geophysics, and Prof. Jan D. Achenbach of Northwestern University, Department of Civil Engineering, Illinois, have been so kind as to provide constructive criticisms of the manuscript. They suggested a number of improvements to the presentation, for which the author wishes to express his sincere gratitude.

REFERENCES

Achenbach, J.D., 1973. *Wave Propagation in Elastic Solids,* North-Holland, Amsterdam.

Aki, R. & Richards, P.G., 1980. *Quantitative Seismology,* Freeman, San Francisco, CA.

De Hoop, A.T., 1958. Representation theorems for the displacement in an elastic solid and their application to elastodynamic diffraction theory, *PhD thesis,* Delft University of Technology, Delft, the Netherlands.

De Hoop, A.T., 1960. A modification of Cagniard's method for solving seismic pulse problems, *Appl. Sci. Res.,* **B8,** 349–356.

De Hoop, A.T., 1988a. Large-offset approximations in the modified Cagniard method for computing synthetic seismograms, *Geophys. Prospect.,* **36,** 465–477.

De Hoop, A.T., 1988b. Acoustic radiation from impulsive sources in a layered fluid, *Nieuw Archief voor Wiskunde,* **6,** 111–129.

De Hoop, M.V. & De Hoop, A.T., 2000. Wave-field reciprocity and optimization in remote sensing, *Proc. R. Soc. Lond.,* A**456,** 641–682.

Miklowitz, J., 1978. *The Theory of Elastic Waves and Waveguides,* North-Holland, Amsterdam.

Verweij, M.D. & Chapman, C.H., 1999. Transmission and reflection of transient elastodynamic waves at a linear slip interface, *J. acoust. Soc. Am.*, **101,** 2473–2484.
Widder, D.V., 1946. *The Laplace Transform,* Princeton University Press, Princeton, NJ.

APPENDIX A: TIME-DOMAIN EXPRESSIONS FOR THE HALF-PLANE KIRCHHOFF DIFFRACTION FUNCTIONS: FIRST AND SECOND BOUNDARY VALUE PROBLEMS

In this appendix the time-domain expressions corresponding to

$$\hat{D}^{\mathrm{I}}_{\mathrm{K}}(x,z,s)=\frac{1}{2\pi\mathrm{i}}\int_{p=-\mathrm{i}\infty}^{\mathrm{i}\infty}\frac{\gamma_0}{\gamma_S(p)}\frac{1}{p-p_0}\exp\{-s[px+\gamma_S(p)|z|]\}\,dp$$
$$\text{for } \mathscr{R}e(p_0)>0 \tag{A1}$$

(see eq. 53) and

$$\hat{D}^{\mathrm{II}}_{\mathrm{K}}(x,z,s)=\mathrm{sign}(z)\frac{1}{2\pi\mathrm{i}}\int_{p=-\mathrm{i}\infty}^{\mathrm{i}\infty}\frac{1}{p-p_0}\exp\{-s[px+\gamma_S(p)|z|]\}dp$$
$$\text{for } \mathscr{R}e(p_0)>0 \tag{A2}$$

(see eq. 54) are determined with the aid of the modified Cagniard method.

As stipulated in Section 6, the principal step consists of replacing the original path of integration in the complex p-plane (the imaginary axis) by a path along which the exponential functions in the integrands take the form $\exp(-s\tau)$, where τ is a real variable of integration. In the present case, the modified path of integration is defined through

$$px+\gamma_S(p)|z|=\tau\,, \tag{A3}$$

in which τ is a real positive parameter. From eq. (A3) it follows that the required modified path is given by $\{p=p_S\}\cup\{p=p_S^*\}$, where

$$p_S=\frac{x\tau}{R^2}+\mathrm{i}\,\frac{|z|}{R^2}\left(\tau^2-\frac{R^2}{c_S^2}\right)^{1/2}\quad\text{for } R/c_S\le\tau<\infty\,, \tag{A4}$$

with

$$R=(x^2+z^2)^{1/2} \tag{A5}$$

as the distance from the diffracting edge $\{x=0,\ -\infty<y<\infty,\ z=0\}$ to the point of observation and where the asterisk denotes the complex conjugate. Eq. (A4) represents a hyperbolic arc in the upper half of the complex p-plane that intersects the real p-axis at the point $p=(x/R)c_S^{-1}$ at the parameter value $\tau=T_S$, where

$$T_S=R/c_S\,. \tag{A6}$$

The relevant point of intersection always lies in the interval $-c_S^{-1}\le p\le c_S^{-1}$ and to the left of p_0 for $x/R<p_0c_S$ but to the right of p_0 for $x/R>p_0c_S$, whereas for $x/R=p_0c_S$ the modified path of integration would intersect the real p-axis at the pole $p=p_0$. Since under the latter circumstance Cauchy's theorem would no longer apply, the modified path is taken to consist of the relevant cut hyperbolic arc supplemented with a semi-circular arc to the left with its centre at $p=p_0$ and a vanishingly small radius. The three cases are shown in Figs A1, A2 and A3, respectively. Obviously, T_S is the *SH*-wave traveltime from the diffracting edge to the point of observation.

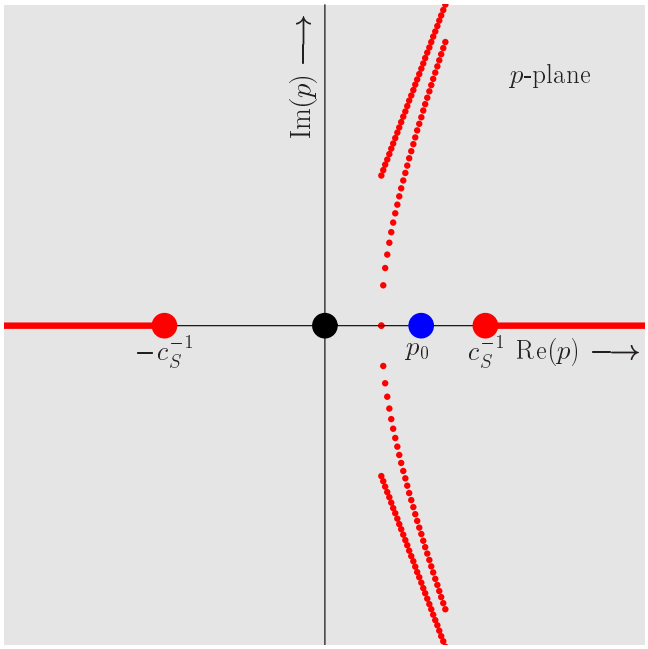

Figure A1. Modified Cagniard path, with asymptote, in the complex slowness plane.

In all three cases, the contribution from the pole can be interpreted as the *ray-geometrical contribution* (that is, the contribution in accordance with geometrical ray theory) to the scattered wave, and the contribution from the hyperbolic arcs as the *diffraction contribution* to the scattered wave. In the expressions for the latter, the contributions from $p=p_S$ and $p=p_S^*$ are combined under the application of Schwarz's

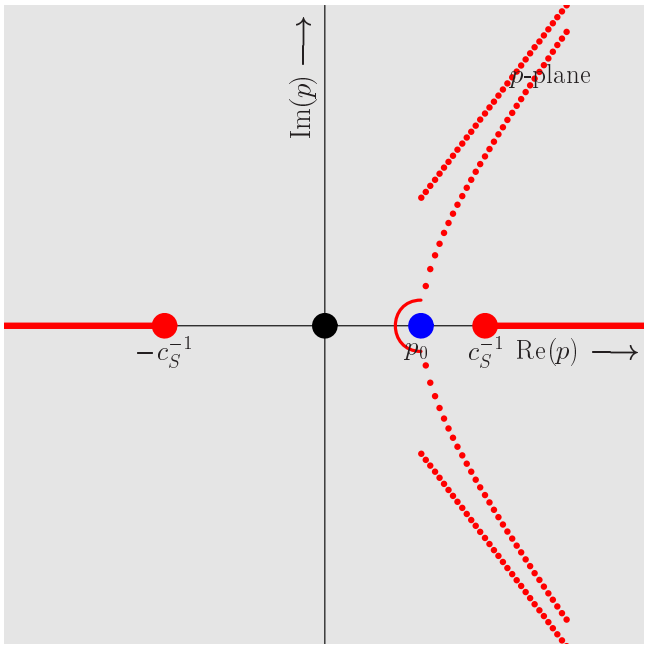

Figure A2. Modified Cagniard path, with asymptote and semi-circular arc around the pole p_0, in the complex slowness plane.

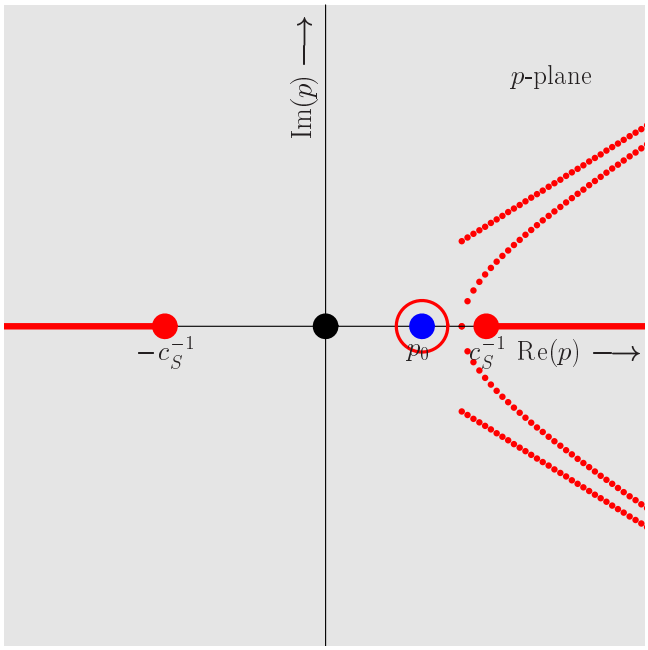

Figure A3. Modified Cagniard path, with asymptote and circular arc around the pole p_0, in the complex slowness plane.

reflection principle of complex function theory and τ is introduced as the variable of integration. The Jacobian of the change in the variable of integration follows from eq. (A4) as

$$\frac{\partial p_S}{\partial \tau} = \frac{\mathrm{i}|z|\tau}{R^2}\left(\tau^2 - \frac{R^2}{c_S^2}\right)^{-1/2} + \frac{x}{R^2}\,, \tag{A7}$$

which, with

$$\gamma_S(p_S) = \frac{|z|\tau}{R^2} - \mathrm{i}\,\frac{x}{R^2}\left(\tau^2 - \frac{R^2}{c_S^2}\right)^{1/2}\,, \tag{A8}$$

can be rewritten as

$$\frac{\partial p_S}{\partial \tau} = \frac{\mathrm{i}\gamma_S(p_S)}{(\tau^2 - R^2/c_S^2)^{1/2}}\,. \tag{A9}$$

Under these operations, eq. (A1) is replaced by

$$\hat{D}_{\mathrm{K}}^{\mathrm{I}} = \hat{D}_{\mathrm{K}}^{\mathrm{I;ray}} + \hat{D}_{\mathrm{K}}^{\mathrm{I;d}}\,, \tag{A10}$$

with the ray-geometrical contribution

$$\hat{D}_{\mathrm{K}}^{\mathrm{I;ray}} = -\left\{0,\ \frac{1}{2},\ 1\right\}\exp\left[-s(p_0 x + \gamma_0|z|)\right]$$

$$\text{for } \{x/R < p_0 c_S,\ x/R = p_0 c_S,\ x/R > p_0 c_S\} \tag{A11}$$

and the diffraction contribution

$$\hat{D}_{\mathrm{K}}^{\mathrm{I;d}} = \frac{1}{\pi}\int_{\tau=T_S}^{\infty}\exp(-s\tau)\mathscr{R}e\left[\frac{\gamma_S(p_S)}{p_S - p_0}\right]\frac{1}{(\tau^2 - T_S^2)^{1/2}}\,d\tau\,, \tag{A12}$$

while eq. (A2) is replaced by

$$\hat{D}_{\mathrm{K}}^{\mathrm{II}} = \hat{u}_{\mathrm{K}}^{\mathrm{II;ray}} + \hat{u}_{\mathrm{K}}^{\mathrm{II;d}}\,, \tag{A13}$$

with the ray-geometrical contribution

$$\hat{D}_{\mathrm{K}}^{\mathrm{II;ray}} = -\mathrm{sign}(z)\left\{0,\ \frac{1}{2},\ 1\right\}\exp\left[-s(p_0 x + \gamma_0|z|)\right]$$

$$\text{for } \{x/R < p_0 c_S,\ x/R = p_0 c_S,\ x/R > p_0 c_S\} \tag{A14}$$

and the diffraction contribution

$$\hat{D}_{\mathrm{K}}^{\mathrm{II;d}} = \mathrm{sign}(z)\,\frac{1}{\pi}\int_{\tau=T_S}^{\infty}\exp(-s\tau)\mathscr{R}e\left[\frac{\gamma_0}{p_S - p_0}\right]\frac{1}{(\tau^2 - T_S^2)^{1/2}}\,d\tau\,. \tag{A15}$$

Application of elementary rules of the one-sided Laplace transformation to the ray-geometrical contributions and of Lerch's theorem to the diffracted contributions finally yields

$$D_{\mathrm{K}}^{\mathrm{I}} = D_{\mathrm{K}}^{\mathrm{I;ray}} + D_{\mathrm{K}}^{\mathrm{I;d}}\,, \tag{A16}$$

with the ray-geometrical contribution

$$D_{\mathrm{K}}^{\mathrm{I;ray}} = -\left\{0,\ \frac{1}{2},\ 1\right\}\delta(t - p_0 x - \gamma_0|z|)$$

$$\text{for } \{x/R < p_0 c_S,\ x/R = p_0 c_S,\ x/R > p_0 c_S\} \tag{A17}$$

and the diffraction contribution

$$D_{\mathrm{K}}^{\mathrm{I;d}} = \frac{1}{\pi}\,\mathscr{R}e\left[\frac{\gamma_S(p_S)}{p_S - p_0}\right]\frac{1}{(\tau^2 - T_S^2)^{1/2}}\,H(t - T_S)\,, \tag{A18}$$

and

$$D_{\mathrm{K}}^{\mathrm{II}} = D_{\mathrm{K}}^{\mathrm{II;ray}} + D_{\mathrm{K}}^{\mathrm{II;d}}\,, \tag{A19}$$

with the ray-geometrical contribution

$$D_{D}^{\mathrm{II;ray}} = -\mathrm{sign}(z)\left\{0,\ \frac{1}{2},\ 1\right\}\delta(t - p_0 x - \gamma_0|z|)$$

$$\text{for } \{x/R < p_0 c_S,\ x/R = p_0 c_S,\ x/R > p_0 c_S\} \tag{A20}$$

and the diffraction contribution

$$D_{\mathrm{K}}^{\mathrm{II;d}} = \mathrm{sign}(z)\,\frac{1}{\pi}\,\mathscr{R}e\left[\frac{\gamma_0}{p_S - p_0}\right]\frac{1}{(\tau^2 - T_S^2)^{1/2}}\,H(t - T_S)\,. \tag{A21}$$

These results are used in the main text.